

# Compatibility of the CO and HI linewidths considering the gas distribution and rotation curves

Y. Tutui and Y. Sofue

Institute of Astronomy, University of Tokyo, Mitaka Tokyo 181-8588, Japan

Received 23 June 1998 / Accepted 25 May 1999

**Abstract.** We have found the trend between CO and HI linewidths by compiling the CO and HI linewidths of 219 nearby galaxies. The trend is that the CO linewidths of fast rotating galaxies tend to be larger than the HI linewidths, and that the HI linewidths of slow rotating galaxies tend to be larger than the CO linewidths, whereas the intermediately rotating galaxies have almost equal values. We have examined the trend using the synthetic rotation curve model given by Persic et al. (1996), which provides the linewidth – absolute magnitude relations at any radii. We conclude that the trend is produced by the differences in CO and HI distributions in a galaxy and the gradient of a rotation curve that depends on the luminosity of the galaxy. We should note that the distribution of the tracer of linewidths (e.g. CO, HI) and the gradient of rotation curves influence observed linewidths, therefore the exact linewidths should be corrected for them.

**Key words:** cosmology: distance scale – galaxies: distances and redshifts – galaxies: general – galaxies: ISM – radio lines: galaxies

## 1. Introduction

The HI linewidth – luminosity relation (hereafter the HI TF relation) has been one of the most successful and widely applied methods to determine distances to galaxies up to  $cz \sim 10,000 \text{ km s}^{-1}$ , or  $100h^{-1} \text{ Mpc}$  (e.g. Tully & Fisher 1977, Aaronson et al. 1986, Pierce & Tully 1988). HI observations with a single dish telescope for the HI TF relation beyond this redshift have been affected by the source confusion and the signal dilution due to the larger beam size. For farther galaxies beyond the HI limit ‘the CO TF relation’ using CO linewidths instead of HI is available (Dickey & Kazes 1992, Sofue 1992). It is advantageous for higher  $cz$  galaxies, because the beam size in CO observations is sharper than HI, also there are a lot of samples that have higher CO luminosity. The compatibility of CO and HI linewidths was examined and showed good agreement for nearby spiral galaxies (e.g. Dickey & Kazes 1992, Schöniger & Sofue 1994,

Schöniger & Sofue 1997, Lavezzi & Dickey 1998). In the case of interacting galaxies both linewidths are affected by the interaction, the CO linewidth is stable enough to apply the TF relation for weakly interacting galaxies (Tutui & Sofue 1997).

The distributions of CO and HI in a galaxy are clearly separated and the boundary is known as the molecular front (Sofue et al. 1995, Honma et al. 1995). The rotation curves are not completely flat and the shape and amplitude depend on the size of a galaxy or luminosity (e.g. Sancisi & van Albada 1987, Persic et al. 1996). Besides the CO and HI linewidths are given by the rotation velocity where the gas is distributed. This means the relation between CO and HI linewidths depends on the size or luminosity of the galaxy. We discuss the CO and HI distributions with a synthetic rotation curve model presented by Persic et al. (1996).

In this paper we present the data and sample selection in Sect. 2, the comparison between CO and HI linewidths and the analysis based on the rotation curve model given by Persic et al. (1996) in Sect. 3, the discussion of the methods that we used for the analysis and the summary in Sect. 4.

## 2. Data and sample selection

We have sampled the  $^{12}\text{CO}(J = 1 - 0)$  linewidth data from some catalogs of nearby galaxies. Although some of these CO linewidths are measured by a single beam that is sufficient to cover the extent of CO, most are synthesized from mapping along the major axis. For the latter case we have estimated the linewidths from the position – velocity diagram. This method may diminish the correlation with the HI linewidths that are observed with the single beam. This effect is discussed in the last section. The properties of the CO data are listed in Table 1. We have compiled the HI linewidths and the inclination using the LEDA (Lyon - Meudon Extragalactic Database). From the original sample we have excluded (1) face-on galaxies of  $i < 30^\circ$  and (2) morphologically interacting galaxies. The number of galaxies after these selections is listed in Column 2 in Table 1. The linewidths are defined as the full width at 20% of the maximum intensity and corrected for the inclination:  $W_{i \text{ CO}}$  ( $= W_{\text{CO}} / \sin i$ ) and  $W_{i \text{ HI}}$  ( $= W_{\text{HI}} / \sin i$ ) for CO and HI, respectively.

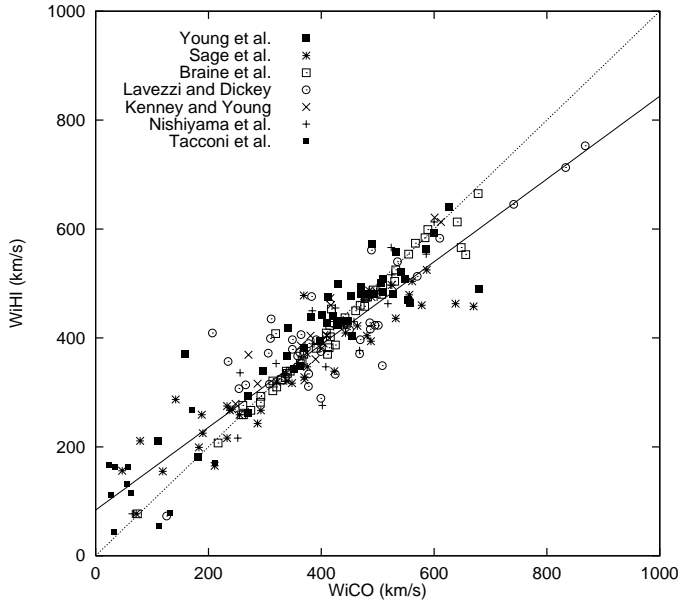


**Fig. 1.** Plot of the linewidths of CO and HI. The face-on galaxies whose inclination is less than 30deg have been excluded, and the linewidths are corrected for the inclination. The references of each symbol are listed in Table 1. The solid line is obtained by the least square fit of the whole sample.

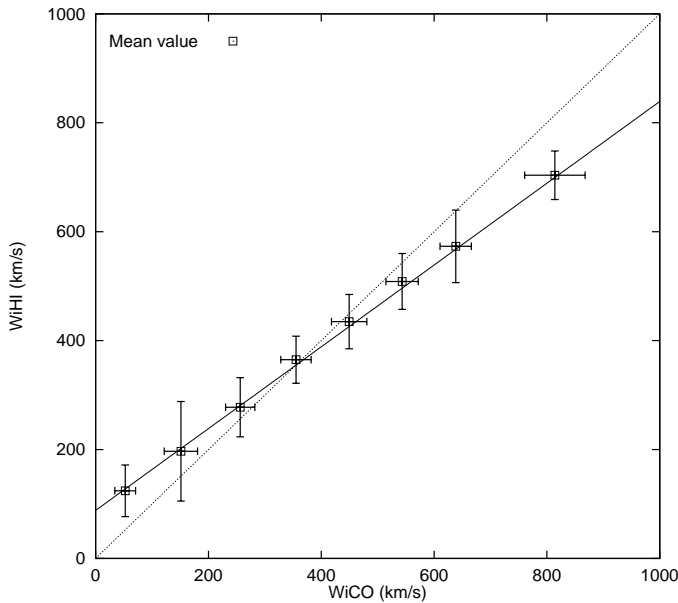


**Fig. 2.** Means and the standard deviations for each bin of the portion of the CO linewidths. The properties of the bins are listed in Table 2. The solid line is the same fitted line as Fig. 1.

### 3. Results

#### 3.1. A trend between CO and HI linewidths

We re-examined the CO and HI linewidths relation as Dickey & Kazes (1992) and Schöniger & Sofue (1992) did, with larger samples. The samples that we used here were selected from slow rotating galaxies to fast rotating galaxies listed in Table 1. Fig. 1

**Table 1.** References of the sample and the properties of the CO observations.

Reference	No.	Observatory	HPBW('')
Young et al. 1995	42	FCRAO 14-m	45
Sage 1993	39	NRAO 12-m	55
Braine et al. 1993	51	IRAM 30-m	23
Lavezzi & Dickey 1998	39	NRAO 12-m	55
Kenney & Young 1988	16	FCRAO 14-m	45
Nishiyama 1995	21	NRO 45-m	15
Tacconi & Young 1987	11	FCRAO 14-m	45

**Table 2.** Properties of the portion of the CO linewidths in each bin.

Range	No.	Y95	S93	B93	L97	K88	N95	T87
0–100	12	0	3	1	0	0	1	7
100–200	12	3	5	0	1	0	0	3
200–300	28	3	8	7	4	3	2	1
300–400	52	7	7	14	16	5	3	0
400–500	66	16	8	17	10	6	9	0
500–600	34	11	6	8	4	0	5	0
600–700	12	2	2	4	1	2	1	0
700–900	3	0	0	0	3	0	0	0
total	219	42	39	51	39	16	21	11

*Column 1:* Range of the CO linewidth of each bin. The linewidth are corrected for the inclination. *Column 2:* The number of galaxies in each bin. *Columns 3–9:* Distribution of the number of galaxies for each reference: Young et al. 1995 (Y95), Sage 1993 (S93), Braine et al. 1993 (B93), Lavezzi & Dickey 1998 (L98), Kenney & Young 1988 (K88), Nishiyama 1995 (N95) and Tacconi & Young 1987 (T87).

is the plot of CO linewidths against corresponding HI linewidths whose inclinations have been corrected. We see from Fig. 1 that the values of both CO and HI linewidths are not entirely equivalent, but HI linewidths are broader than CO for slow rotating galaxies (*i.e.* dwarf galaxies) and CO linewidths are broader than HI for fast rotating galaxies (*i.e.* massive galaxies). We fitted the samples by the least square method, and obtained the relation, that is shown as the solid line in Fig. 1:

$$W_{i \text{ HI}} = 0.76W_{i \text{ CO}} + 83.8. \quad (1)$$

We divided the samples into eight bins of the portion of the CO linewidths. The contents of the bins are listed in Table 2. We evaluated the mean value and the standard deviation in each bin and showed them in Fig. 2. Fig. 2 indicates the following: (1) The subsamples of each bin obey the best fit relation (Eq. (1)) very well through the whole linewidth. (2) For intermediately rotating galaxies whose linewidth is about between 300 km s<sup>-1</sup> and 600 km s<sup>-1</sup>, CO and HI linewidths correspond very well within the small dispersion. (3) The large dispersions of slow rotating galaxies are caused by not only the small samples but also the difficulties in measuring the linewidths. As Giovanelli et al. (1997) indicated, we see that the dispersion in linewidths for the small rotating galaxies increases toward the smaller linewidths, whereas the dispersion for the intermediately to fast rotating galaxies is almost constant.

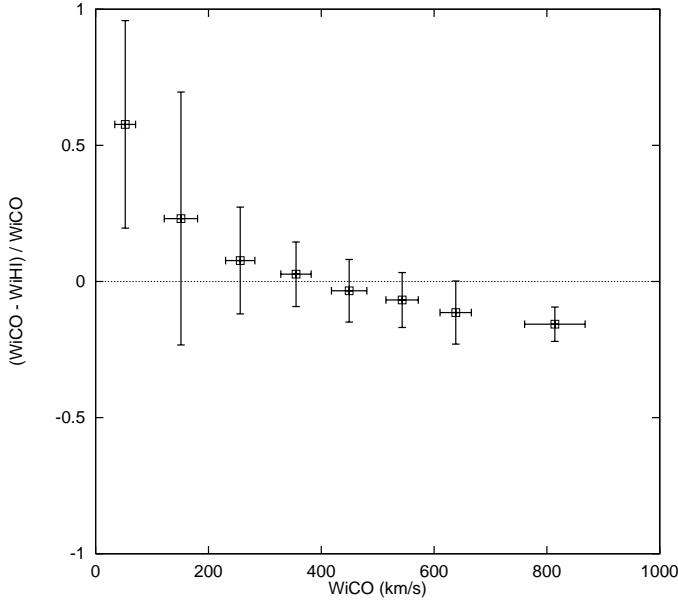


**Fig. 3.** Residual between CO and HI linewidths that is normalized by the CO linewidths noted as  $(W_{i\text{ HI}} - W_{i\text{ CO}})/W_{i\text{ CO}}$ , against the CO linewidths for each bin. The normalization by the linewidth is useful to evaluate the effect of the difference after applying the TF relation.

In the case of applying a linewidth into the TF relation, the estimated absolute magnitude differs as a function of the logarithm of the linewidth, therefore the comparison of both linewidths for the effect of the TF relation should be taken as the ratio. Fig. 3 shows the residuals of both linewidths as the notation of  $(W_{i\text{ HI}} - W_{i\text{ CO}})/W_{i\text{ CO}}$  in each bin. This shows that slow rotating galaxies are not a good sample when applying the TF relation, we should also note that the observed rotation velocity in CO and HI provide different values.

### 3.2. Synthetic rotation curves and the TF relation

Fig. 4 shows the CO data distribution in each bin over the TF (linewidth – absolute magnitude) diagram. Here the absolute magnitude is calculated by the *I*-band TF relation given by Pierce & Tully (1992):

$$M_I = -8.72(\log W_i - 2.50) - 20.94. \quad (2)$$

As we showed the difference in the CO and HI linewidths in the previous section, the most appropriate TF relation with the CO linewidths is shifted from the HI TF relation for the slow rotating galaxies and the fast rotating galaxies. This effect also appears in Fig. 4. The TF relation connected by the CO data points is different from the HI TF relation. The connected CO TF relation, except the slowest rotation portion, shows a linear relation like the HI TF relation. While it provides the different values of the slope and offset from the HI TF relation, the output absolute magnitudes from both TF relations do not vary much for the intermediately rotating galaxies. It suggests that the CO and HI linewidths are compatible for the intermediately rotating galaxies, whereas the fast and slow rotating galaxies have different values.

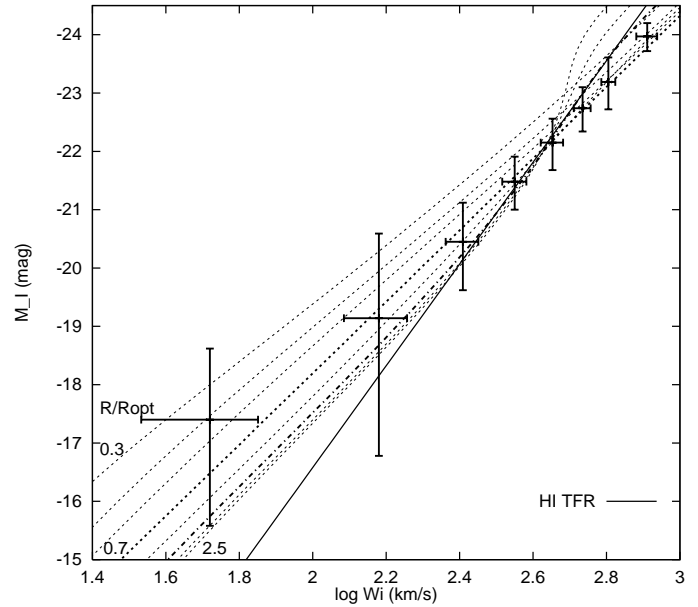


**Fig. 4.** Linewidth – absolute magnitude diagram: The crosses are the CO data bin indicated in Table 2, and their absolute magnitudes are estimated by the *I*-band TF relation of Eq. (2), which is drawn as the solid line. If a CO linewidth is equal to a corresponding HI linewidth, the expected values of the absolute magnitude should be put on the line of the HI TF relation. The dotted lines show the specific radii of the PSS model, for  $R/R_{opt} = 0.3, 0.4, 0.5, 0.7$  (thick dotted line), 1.0, 1.5 (thick dotted broken line), 2.0 and 2.5, from top to bottom.

In order to discuss the difference between the two TF relations, we used the synthetic rotation curve model, that is based on the statistics of rotation curves, proposed by Persic et al. (1996) (hereafter the PSS model). According to the PSS model the rotation velocity is a function of not only the radius but also the luminosity. The three variables in the PSS model are (1) rotation velocity,  $V_{rot}$ , (2) absolute magnitude in the *I*-band,  $M_I$  and (3) the galacto-centric radius normalized by the optical disk radius,  $R/R_{opt}$ . They make a surface in a three-dimensional space<sup>1</sup> (i.e.  $V_{rot} - M_I - R/R_{opt}$ ). Here,  $R_{opt}$  corresponds to the de Vaucouleurs 25  $B_{mag}$  mag arcsec<sup>-2</sup> photometric radius for the Freeman disk, or corresponds to 3.2  $R_d$  for the exponential surface brightness distribution, where  $R_d$  is the disk scale length. This surface is useful to discuss the rotation curves and the TF relation, because they are obtained by the projection of the surface. If the surface is projected onto the  $V_{rot}$  vs.  $R/R_{opt}$  plane, it shows the synthetic rotation curves, that is called ‘the universal rotation curves’ by PSS96, with the parameter of the absolute magnitude  $M_I$  (See dotted lines in Fig. 5.). On the other hand, if the surface is projected onto the  $V_{rot}$  vs.  $M_I$  plane, it shows a kind of TF relation (linewidth – luminosity relation) with the parameter of the specific radius  $R/R_{opt}$ . (See dotted line in Fig. 4.) The values of the specific radius are shown as the dotted lines of  $R/R_{opt} = 0.3, 0.4, 0.5, 0.7$  (thick dotted line), 1.0, 1.5 (dotted broken line), 2.0 and 2.5, top to bottom. Here we

<sup>1</sup> See Fig. 10 in Persic et al. 1996

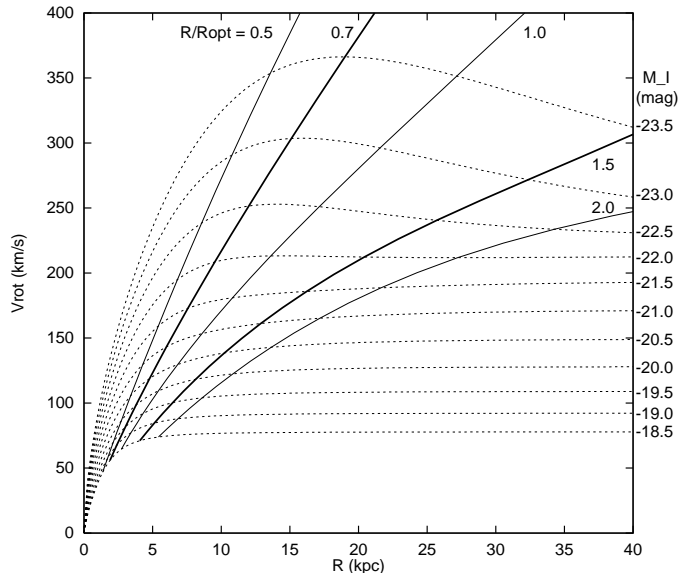


**Fig. 5.** Isoradius curves of the specific radius,  $R/R_{opt}$ , over the rotation curves of the PSS model. The values of  $R/R_{opt} = 0.5, 0.7$  (thick line), 1.0 and 1.5 (thick line) are displayed.

have defined the linewidths as twice the rotation velocity used in the PSS model.

In Fig. 4 the comparison between the PSS model and the HI TF relation shows the following: (1) The HI TF relation does not fit the PSS model in the slow rotation part ( $\log W_i \lesssim 2.3$  km s<sup>-1</sup>). This is consistent with suggestion by Giovanelli et al. (1997) that the HI TF relation is not a good tracer for slow rotating galaxies. (2) The HI TF relation fits the PSS model of around  $R/R_{opt} \sim 1.5$  well. This is consistent with the HI distribution in a galaxy, where it is extended over the optical radius. (3) On the other hand, the CO data points trace the inner radius of the PSS model than the optical radius through the whole linewidth. This is also consistent the CO distribution in a galaxy.

#### 4. Discussion and summary

The results that we discussed in the previous section can be explained by how the distributions of CO and HI differ and how the rotation curves depend on the luminosity. Fig. 5 indicates the specific isoradius curves of  $R/R_{opt}$  over the synthetic rotation curves using the PSS model. Rotation curves observed by optical spectroscopy are within the radius of  $R/R_{opt} \sim 1.0$ . We have found that the specific radius for the CO data is about  $R/R_{opt} \sim 0.7$ , where the rotation curves trace the maximum velocity part of the disk component, whereas, for the HI linewidths, it is about  $R/R_{opt} \sim 1.5$  and it traces the outer rather flatter part of the rotation curves. We should pay attention to the difference between them when we discuss the rotation velocity or the TF relation in CO and in HI. The PSS model is constructed from the statistics of rotation curves and by fitting of two mass components, a disk and a halo. We should note that the PSS model does not follow the real rotation curves in the central region. Sofue et

al. (1999) have discussed the central rotation curves, and found that most rotation curves, except for dwarf galaxies, are almost flat towards the center or show a nucleus high velocity part for some fast rotating galaxies. The bulge and nucleus components are not considered in the PSS model, as the influence of these components on the rotation curves is small for this analysis at  $R/R_{opt} \gtrsim 0.5$ .

The CO linewidths which we used in this analysis are estimated by the position – velocity diagrams which are observed along the major axis, except Lavezzi & Dickey’s (1998) sample that has larger  $cz$  enough to cover the CO extent in a single beam. On the contrary, the HI linewidths are measured by the single beam. It may cause the bias for the relation between the CO and HI linewidths. Mapping along the major axis may not cover the real linewidth. In order to avoid the bias we have excluded the face-on galaxies.

In summary, we have found the trend between the CO and HI linewidths by compiling the CO and HI datasets. HI linewidths are larger than CO for slow rotating galaxies, and CO linewidths are larger than HI for fast rotating galaxies. This trend is common through out all datasets, although the slow rotating portion has a large dispersion. The linewidths for slow rotating galaxies of  $W_i \lesssim 300$  km s<sup>-1</sup> are not appropriate when applying the TF relation. Although the trend gives a different slope and offset values for the TF relation from those of HI, the output absolute magnitude of intermediately rotating galaxies of  $300 \text{ km s}^{-1} \lesssim W_i \lesssim 600 \text{ km s}^{-1}$  is approximately equivalent to that provided by the HI TF relation.

In order to explain the trend we have examined the synthetic rotation curve model proposed by Persic et al. (1996). The trend can thus be explained by both the different distributions of the CO and HI in a galaxy and the entirely non-flatness of the rotation curves. Combining the TF relation with the synthetic rotation curves of the PSS model shows that the radius within the optical radius where CO is distributed is reflected in the CO linewidths, and the radius beyond the optical radius where HI is distributed is also reflected in the HI linewidths. It is worth noting that the distribution of CO, HI or anything else used in measuring the linewidths actually influences the linewidths, therefore the exact linewidths should be corrected for the effects of the rotation curves and the gas distribution.

*Acknowledgements.* The author *YT* acknowledges the financial support by the Research Fellowships of the Japan Society for the Promotion of Science for Young Scientists. This research made use of the Lyon/Meudon Extragalactic Database (LEDA).

#### References

- Aaronsen M., Bothun G., Mould J., et al., 1986, ApJ 302, 536
- Braine J., Combes F., Casoli F., et al., 1993, A&AS 97, 887
- Dickey J.M., Kazes I., 1992, ApJ 393, 530
- Giovanelli R., Haynes M.P., Herter T., et al., 1997, AJ 113, 53
- Honma M., Sofue Y., Arimoto N., 1995, A&A 304, 1
- Kenney J.D., Young J. S., 1988, ApJS 66, 261
- Lavezzi T.E., Dickey J.M., 1998, AJ 116, 2672
- Nishiyama K., 1995, In: The thesis of the Graduate University for Advanced Studies

- Persic M., Salucci P., Stel F., 1996, MNRAS 281, 27 (PSS96)
- Pierce M.J., Tully R.B., 1988, ApJ 330, 579
- Pierce M.J., Tully R.B., 1992, ApJ 387, 47
- Sage L.J., 1993, A&AS 100, 537
- Sancisi R., van Albada T.S., 1987, In: Kormendy J., Knapp G.R. (eds.)  
Dark Matter in the Universe. IAU Symposium No. 117, Reidel,  
Dordrecht, p. 67
- Schöniger F., Sofue Y., 1994, A&A 283, 21
- Schöniger F., Sofue Y., 1997, A&A 323, 14
- Sofue Y., 1992, PASJ 44, L231
- Sofue Y., Honma M., Arimoto N., 1995, A&A 296, 33
- Sofue Y., Schoniger F., Honma M., et al., 1996, PASJ 48, 657
- Sofue Y., Tutui Y., Honma M., et al., 1999, ApJ in press
- Tacconi L.J., Young J.S., 1987, ApJ 322, 681
- Tully R.B., Fisher J.R., 1977, A&A 54, 661
- Tutui Y., Sofue Y., 1997, A&A 326, 915
- Young J.S., Xie S., Tacconi L., et al., 1995, ApJS 98, 219